

# Femtosecond Dynamics in Single Wall Carbon Nanotube/Poly(3-Hexylthiophene) Composites

Emmanouil Lioudakis · Andreas Othonos ·  
Ioannis Alexandrou

Received: 12 April 2008 / Accepted: 11 July 2008 / Published online: 29 July 2008  
© to the authors 2008

**Abstract** Femtosecond transient absorption measurements on single wall carbon nanotube/poly(3-hexylthiophene) composites are used to investigate the relaxation dynamics of this blended material. The influence of the addition of nanotubes in polymer matrix on the ultrashort relaxation dynamics is examined in detail. The introduction of nanotube/polymer heterojunctions enhances the exciton dissociation and quenches the radiative recombination of composites. The relaxation dynamics of these composites are compared with the fullerene derivative-polymer composites with the same matrix. These results provide explanation to the observed photovoltaic performance of two types of composites.

**Keywords** Ultrafast spectroscopy ·  
Single wall carbon nanotubes · Exciton dissociation

## Introduction

The last two decades, the optical properties of single wall carbon nanotubes (SWNTs) have gained a great deal of interest [1–3]. The one-dimensional (1D) nature of nanotubes offers unique properties to their excitonic spectrum with many revolutionary applications [4, 5]. Many experimental techniques such as Raman scattering and electrical conductivity [6] have been employed for the investigation of optical and electronic properties of nanotubes with

variable diameters and angle chiralities [7, 8]. Relaxation dynamics and nonlinear properties in these nanostructures are key issues in understanding and developing their optoelectronic properties. Ultrafast studies of carrier dynamics have been performed in SWNTs [9] reporting that this system has a dynamic response ( $<1$  ps) one order of magnitude slower than in graphite ( $\sim 130$  fs) [10]. When mixing the SWNTs with conjugated polymers, the donor/acceptor interfaces of polymer/nanotube act as dissociation heterojunctions for photoexcited excitons. These bulk heterojunction structures are presently believed to be the best approach for organic photovoltaics [11] and the advantage of this photoinduced charge generation [12] is evident with the enhancement of photocurrent in organic solar cells [4, 13]. Particularly,  $\pi$ -conjugated poly(3-hexylthiophene) (P3HT) has been of interest because of high carrier mobility, mechanical strength, thermal stability, and compatibility with fabrication process. However, the literature is lacking a comprehensive study of exciton and dissociated carrier (polarons and electrons) dynamics in these very promising composites for photovoltaic and optoelectronic applications.

In this letter, transient absorption measurements [14, 15] with femtosecond resolution ( $\sim 150$  fs) [16] provides a means to investigate the ultrafast electron transfer from conjugated polymer to nanotubes and the involved radiative or nonradiative relaxations. We resolve the relaxation of excitons and dissociated carriers in SWNT/P3HT composites as a function of nanotube concentration. We have found that carrier relaxation within the valence and conduction bands of P3HT is beyond our resolution time ( $\sim 150$  fs) whereas the exciton dynamics have a double exponential relaxation. Furthermore, the electron–phonon interactions at the vibronic sidebands quench the radiative emission by introducing nonradiative relaxation channels.

E. Lioudakis (✉) · A. Othonos  
Department of Physics, Research Center of Ultrafast Science,  
University of Cyprus, P.O. Box 20537, 1678 Nicosia, Cyprus  
e-mail: mlioud@ucy.ac.cy

I. Alexandrou  
Electrical Engineering and Electronics, University of Liverpool,  
Liverpool L69 3GJ, UK

In addition, based on the observed ultrafast relaxation we present a comparison of SWNTs and [6,6]-phenylC61-butyric acid methyl ester (PCBM) as mixture materials in the P3HT polymer matrix for their photovoltaic performance.

### Experimental Procedure

The utilized experimental technique in this work is a noncollinear super-continuum pump probe configuration in conjunction with a regenerative Ti:Sapphire amplifier system with 100 fs pulses at 800 nm. This system amplifies the pulses to approximately 1 mJ at a repetition rate of 1 kHz. The temporal resolution of our experimental setup over the entire probing wavelength range has been measured to be better than 150 fs. The temporal variation in the optical absorption was monitored as a change in the reflectivity and transmission, which was a direct measure of the photo-excited carrier dynamics within the probing region [17]. In this work, optical pumping at a fluence of  $2 \text{ mJ/cm}^2$  was used to excite the composites and determine their temporal behavior. Here, we should point out that around this fluence nonlinear effects such as exciton–exciton annihilation were not observed in our experimental studies.

For the preparation of the samples in this work, P3HT (5 mg) was dissolved in 10 ml of dichlorobenzene inside a quartz pot which was kept over a hot plate at medium temperature. The initial volume of dichlorobenzene was noted and solvent was added if needed to replenish the evaporated amount. The P3HT solution was gently stirred until all solid P3HT was dissolved. One milligram of HiPCO SWNTs (obtained from CNI) was separately dispersed in 40 ml of dichlorobenzene. HREM (using a JEOL 4000EXII) observations showed that the nanotube material was free from catalytic remnants and formed bundles containing of up to seven nanotubes each. According to current literature, the HiPCO SWNTs are 1/3 metallic and 2/3 semiconducting. We have not performed any additional purification. Appropriate amounts of P3HT and SWNTs were mixed from solution and the composites were ultrasonically agitated so long as to reach a uniform solution. Thin layers of the materials were deposited on quartz substrates by drop casting. The total mass of the deposited materials and the surface of the quartz substrates were kept the same to insure that the resulting films had similar thicknesses. Processing and measurements were performed under ambient conditions.

The dispersion of SWNTs in the composites was examined by HREM using the JEOL 2000EX II microscope and we did not notice any difference compared to the pure SWNTs. In addition,  $I$ – $V$  measurements revealed a

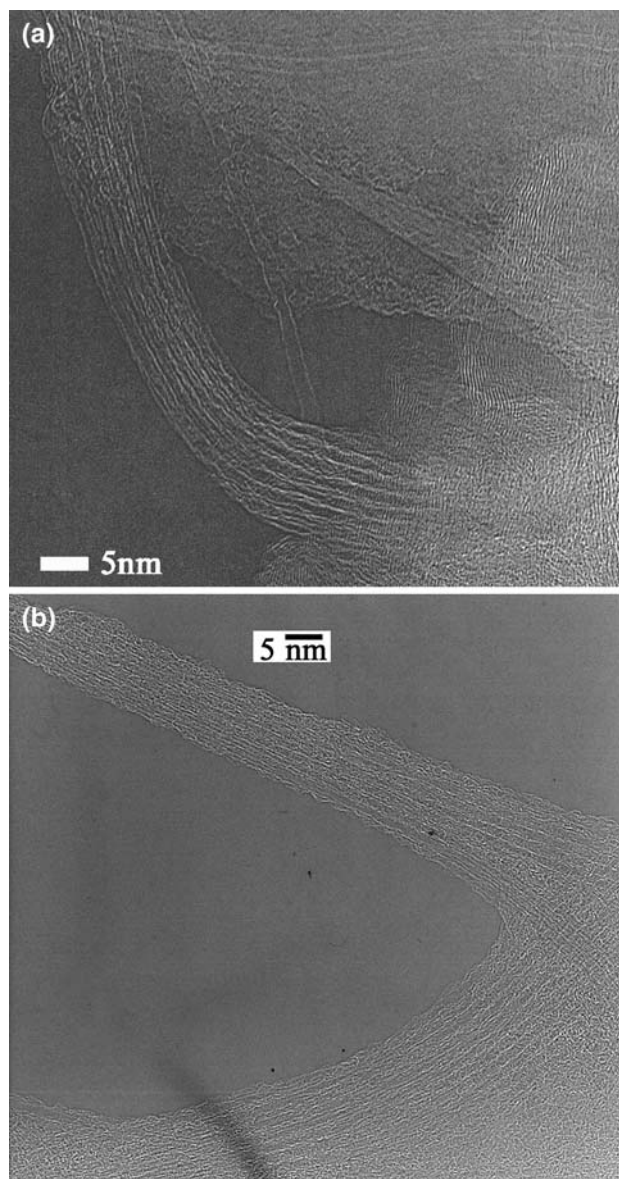


**Fig. 1** High resolution electron microscopy images of (a) pure SWNTs and (b) SWNTs dispersed in P3HT polymer (SWNT concentration 50%)

percolation threshold of 0.75 wt.% which denotes good dispersion of the SWNTs in line with current bibliography [18].

It was clear from these measurements (Fig. 1) that upon increasing the nanotube concentration in our composites, the nanotubes form ropes and bundles with measured nanotube diameters about  $1.4 \pm 0.1 \text{ nm}$ . The effect of the SWNTs bundles formation on the optical excitonic transitions for pure SWNTs material has been experimentally studied [19]. The interactions between SWNTs in close proximity with one another, and the corresponding changes in their electronic structure, have received much attention

[20–23]. In addition to the inherent interest in understanding interacting 1D systems, intertube interactions are of substantial technological importance because SWNTs naturally form bundles in typical syntheses [24] and bundling has the effect of both shifting and broadening the electronic transition energies [25].

## Results and Discussion

In Fig. 2, we present the optical absorption spectrum as a function of wavelength for the pure P3HT polymer and SWNT/P3HT composites. It is obvious that the P3HT polymer absorbs in the visible spectra region depicting a singlet exciton transition (600 nm) and two vibronic sidebands (520 and 560 nm, respectively) [11, 26]. Upon increasing the concentration of nanotubes, the absorbance of the composites decreases (see the inset of Fig. 2).

The decrease in the P3HT absorption is most likely due to the fact that there is less P3HT in the sample (65% SWNT means that only 35% of the sample is P3HT, and the total sample mass is kept constant). Due to various interactions that exist between the two materials (donor–acceptor system) one will expect different relaxation dynamics.

In Fig. 3, we present the experimental data of transient absorption for the pure P3HT polymer when it is excited by ultrashort laser pulses (150 fs) at 400 nm. From these data, it is obvious that when we probe at resonant with the singlet exciton transition (600 nm) we observe a pulse-width limited drop of absorption which is attributed to state filling by

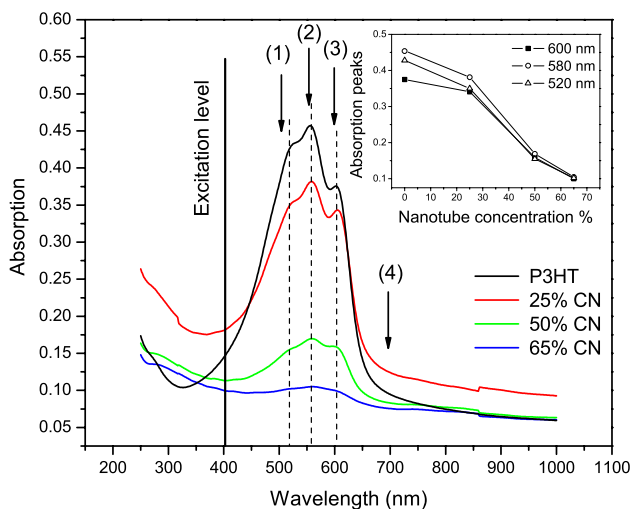


**Fig. 2** Optical absorption measurements at room temperature of SWNT/P3HT composites as a function of wavelength. The *solid line* represents the initial excitation level at 400 nm. The vertical vectors represent the particular probing wavelengths of our transient absorption study. The inset shows the absorption peaks as a function of nanotube concentration at the singlet exciton transition and the vibronic sidebands

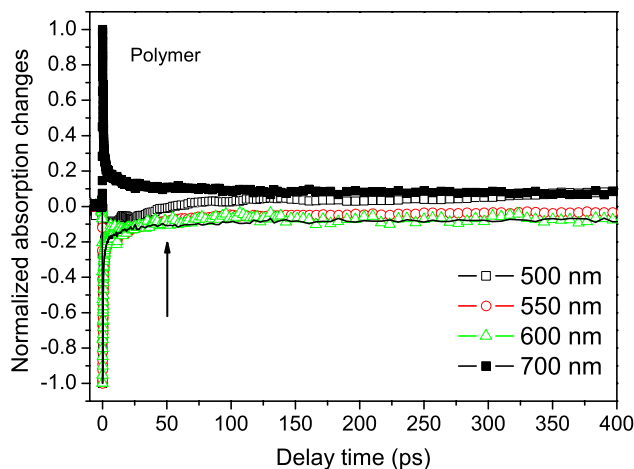


**Fig. 3** Normalized transient absorption measurements for the pure P3HT polymer at probing wavelengths 500, 550, 600, and 700 nm. The inset shows the short scale dynamic behavior. The arrow indicates the time where the signal becomes positive for probing wavelength of 500 nm. The solid black line represents the mirror image of transient absorption signal with probing wavelength of 700 nm for comparison purposes

the Coulomb-correlated electron–hole pairs at the particular probing energy state. This pulse width limited fast drop suggests that the exciton relaxation within the valence and conduction bands of polymer is beyond our time resolution. As the excitons relax, the transient absorption signal increases accordingly. The increased transient absorption behavior can be described by two exponential decays. The first one is fast with a time constant  $<1$  ps and represents the fast relaxation of excitons with energies close to the separation between the Gaussian-like higher occupied molecular orbital (HOMO) and lower unoccupied molecular orbital (LUMO) states. The second decay can be described with a stretched exponential [27] and most likely corresponds to the radiative emission of the P3HT polymer. The latter is more pronounced when we probe very close to resonant with the first or second vibronic sidebands (see the curves of 550 and 500 nm in Fig. 3). At these probing wavelengths, the fast relaxation remains approximately the same, but the second stretched decay becomes faster due to the enhanced coupling of electronic with vibrational states (electron–phonon interactions). This coupling quenches the radiative recombination opening nonradiative relaxation paths by transferring the energy to the lattice via phonons emission.

In addition to monitoring state filling and the subsequent exciton relaxation, the probing beam may cause secondary re-excitations to energetically higher energy states. Secondary absorption probably is present at all probing wavelengths, but it is more pronounced at 550 nm, a wavelength close to the strong second vibronic sideband absorption (see Fig 2). Figure 3 shows transient absorption for a time window of 400 ps. The photoinduced absorption (PA) signal for delay times longer than 50 ps (see 500 nm

probing wavelength in Fig. 3, indicated by an *arrow*) is manifested by the absorption signal becoming positive. Increasing the probing wavelength to 700 nm the energy of the probing photons is less than the HOMO-LUMO energy gap. Since the density of states follows a Gaussian-like distribution there are states in the energy gap which result in weak absorption (see Fig. 2, arrow (4)). Following excitation with the 400 nm laser pulse, we observe an increase in absorption at 700 nm (1.77 eV). This means that we are re-exciting carriers from an energy level that is occupied after the absorption by the excitation photons. The exact location of the involved energy level is not easy to pinpoint. However, if we create a mirror image of the transient absorption at 700 nm with respect to the time delay axis, the resulting curve (shown in Fig. 3 as a continuum black line throughout the data) depict similar dynamics as the 600 nm transient absorption data. This suggests that the 700 nm probe re-excites carriers between the LUMO and a state 1.77 (700 nm) above it (for electrons).

Nanoengineered composites of semiconducting polymers offer opportunities to realize desirable different optical and electronic properties based on exciton energy transfer or dissociation phenomenon across the nano-interface between SWNTs and P3HT. Figure 4 shows the relaxation dynamics of composites when we probe at resonant with the singlet exciton transition of P3HT matrix (600 nm). It is apparent from these data that the donor/acceptor interfaces in composites enhance the dissociation of excitons across the heterojunctions.

Following the initial excitation by the 400 nm photons, the probing 600 nm beam monitors the population of excitons at the energy state located 2 eV above the HOMO. As the nanotube concentration increases, the fast exponential

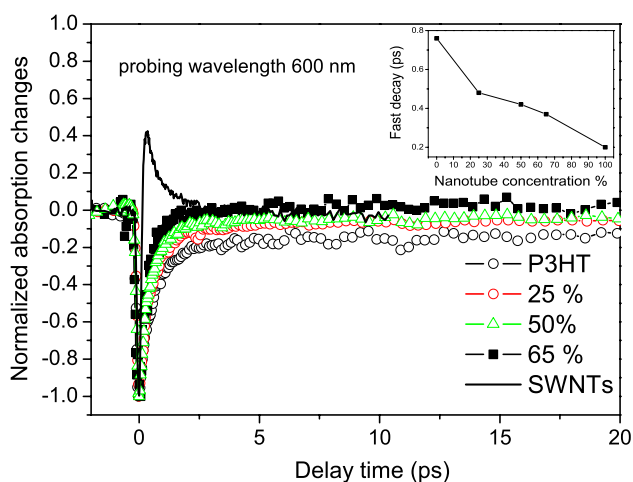


**Fig. 4** Normalized transient absorption measurements for the P3HT polymer, pure SWNTs, and SWNT/P3HT composites at probing wavelength of 600 nm. The inset shows the fast decay time as a function of nanotube concentration

decay becomes progressively faster. This means that excitonic relaxation is indeed enhanced by the presence of nanotubes. We propose that exciton dissociation is amplified at the nanotube-polymer bulk heterojunctions due to the presence of the inherent field at these junctions. From the experimental data in Fig. 4, it is obvious that the nanotubes act as dissociation centers for the excitons minimizing the radiative recombination (smaller stretched decay). The variation in exciton dissociation efficiency can be represented numerically by plotting the fast decay time as a function of nanotube concentration in the inset of Fig. 4. Here, we note that this behavior remains the same for all the probing wavelengths used in this work.

The transient absorption signal of a pure carbon nanotube sample is also shown for comparison in Fig. 4. The signal consists of two contributions: a fast negative transient lasting for a very short period of time and a positive contribution that lasts for the remaining of the measured delay time period. Absorption of the pump pulse ( $\approx 3.1$  eV) creates a population of excitonic states which gradually relax to lower energies before electrons and holes recombine. The fast recovery to positive absorption suggests subsequent secondary excitations by the 600 nm probing wavelength. One cannot be certain the starting (base) and final energy levels involved here, we can only be certain that the energy difference is about 2 eV. In the remaining of delay times, our transient provides an account of the decrease in the population of the base energy level of the re-excitation.

A detail analysis of these two antagonistic contributions for a broad spectrum of probing wavelengths between 480 and 980 nm for pure SWNTs is presented in Fig. 5.

At the probing wavelength of 980 nm (1.26 eV), we only observe the photobleaching of excitonic states. PA,

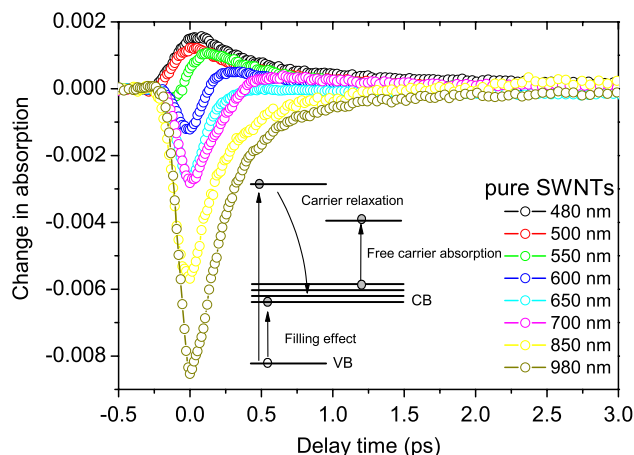


**Fig. 5** Ultrafast transient absorption measurements for pure SWNTs at probing wavelengths ranging between 480 and 980 nm. The inset shows a simple band diagram of carrier relaxation

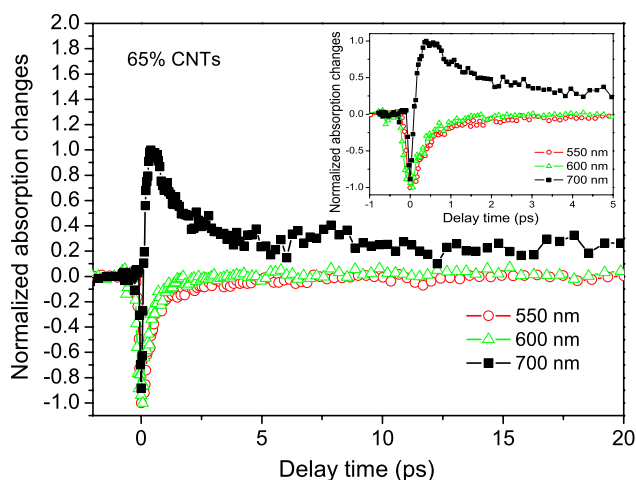


**Fig. 6** Normalized ultrafast transient absorption for the highest concentration composite (65% SWNTs) for probing wavelengths of 550, 600, and 700 nm, respectively. The inset shows a short scale view of these data

however, does not become significant until the probing wavelength becomes 600 nm (2 eV) where we observed delayed PA as described above. Interestingly, for probing wavelengths of 550 nm (2.25 eV) or less, our signal is dominated by PA. As depicted by the simple mechanism depicted in the inset of Fig. 5, PA between states with energy difference between 2 and 2.58 eV is very strong. The dominant negative contribution at lower probing photon energies (between 1.26 and 2 eV) suggests the existence of an almost continuous density of states at these energies. When probing the same behavior in composites with high nanotube concentration (65 wt.%), Fig. 6 shows that the re-excitation at high probing energies (see 550 and 600 nm) is not reproduced. This shows that the pump pulse is predominantly absorbed by the P3HT polymer. The detection of excitonic state populations in SWNTs is therefore completely masked, except for the 700 nm (1.76 eV) probing wavelength where we most likely see a contribution from the SWNTs and the polymer. The initial drop in absorption is due to probing state filling in SWNTs, a trend obvious in Fig. 5. However, the polymer shows a strong PA contribution at 700 nm, a feature we have observed for all composites. Therefore, it is likely that PA contribution sets and overwhelms the negative contribution from the SWNTs absorption.

## Conclusions

In conclusion, we have studied ultrafast transient absorption on P3HT/carbon nanotube composites up to 65% SWNT concentration. Linear absorption measurements in these composites give an important insight of excitonic and vibronic sidebands. The experimental transient absorption

along with the optical absorption measurements reveal that state filling effect and PA take place in these composites. We have found that carrier relaxation within the valence and conduction bands of P3HT is beyond our resolution time ( $\sim 150$  fs) whereas the exciton dynamics have a double exponential relaxation. We have found that the electron–phonon interactions at the vibronic sidebands quench the radiative emission by introducing nonradiative relaxation channels. The addition of nanotubes in these composites alters the relaxation dynamics of formed excitons dissociating these at short time scale and introducing new free-carrier relaxation paths for electrons and polarons through nanotubes and P3HT chains, respectively. Exciton dissociation is accelerated with the concentration of carbon nanotubes strongly suggesting that dissociation takes place at the nanotube–polymer heterojunctions. Furthermore, even at high nanotube concentrations, the pump pulse is predominantly absorbed by the polymer albeit a strong influence by polymer–nanotube heterojunctions on transient absorption of the probe beam. This behavior could be justified by comparing the absorption strength of both materials at 400 nm.

Finally, it is well known in the field of photovoltaic applications that solar cells based on SWNT-P3HT composites do not work well, although SWNT coatings might be useful as transparent electrodes. The evidence in this work suggests that this failing of the SWNTs is not due to lack of exciton dissociation, since we observe shorter exciton lifetimes as the amount of SWNT is increased. This means that maybe other factors, like recombination of charge carriers in nanotubes or polymer chains, are responsible for their poorer performance in these photovoltaics. On the other hand, in preview work [12] we have reported that PCBM-P3HT composites have also a fast exciton dissociation time which quenches the radiative recombination of the polarons/excitons, and increases the yield of photogenerated charged excitations from the PCBM-related states. With increasing the PCBM concentration in the blended materials in that work, we have observed that the relaxation times increase as opposed to the relaxation dynamics upon increasing the SWNT concentration in the same P3HT matrix. We believe that this important difference is responsible for the higher photovoltaic performance of PCBM-P3HT compared with the SWNT-P3HT composite.

**Acknowledgments** The work in this article was partially supported by the research programs ERYAN/0506/04 and ERYNE/0506/02 funded by the Cyprus Research Promotion Foundation in Cyprus.

## References

1. M.S. Dresselhaus, *Nature* **358**, 195 (1992). doi:[10.1038/358195a0](https://doi.org/10.1038/358195a0)
2. S. Iijima, *Nature* **354**, 56 (1991). doi:[10.1038/354056a0](https://doi.org/10.1038/354056a0)

3. M.M.J. Treacy, T.W. Ebbesen, J.M. Gibson, *Nature* **381**, 678 (1996). doi:[10.1038/381678a0](https://doi.org/10.1038/381678a0)
4. E. Kymakis, I. Alexandrou, G.A.J. Amaratunga, *J. Appl. Phys.* **93**, 1764 (2003). doi:[10.1063/1.1535231](https://doi.org/10.1063/1.1535231)
5. E. Kymakis, G.A.J. Amaratunga, *J. Appl. Phys.* **99**, 084302 (2006). doi:[10.1063/1.2189931](https://doi.org/10.1063/1.2189931)
6. E. Kymakis, I. Alexandrou, G.A.J. Amaratunga, *Synth. Met.* **127**, 59 (2002). doi:[10.1016/S0379-6779\(01\)00592-6](https://doi.org/10.1016/S0379-6779(01)00592-6)
7. C.D. Spataru, S. Ismail-Beigi, L.X. Benedict, S.G. Louie, *Phys. Rev. Lett.* **92**, 077402 (2004). doi:[10.1103/PhysRevLett.92.077402](https://doi.org/10.1103/PhysRevLett.92.077402)
8. E. Chang, G. Bussi, A. Ruini, E. Molinari, *Phys. Rev. Lett.* **92**, 196401 (2004). doi:[10.1103/PhysRevLett.92.196401](https://doi.org/10.1103/PhysRevLett.92.196401)
9. J.-S. Lauret, C. Voisin, G. Cassabois, C. Delalande, P. Roussignol, O. Jost et al., *Phys. Rev. Lett.* **90**, 057404 (2003). doi:[10.1103/PhysRevLett.90.057404](https://doi.org/10.1103/PhysRevLett.90.057404)
10. K. Seibert et al., *Phys. Rev. B* **42**, 2842 (1990). doi:[10.1103/PhysRevB.42.2842](https://doi.org/10.1103/PhysRevB.42.2842)
11. E. Lioudakis, A. Othonos, I. Alexandrou, Y. Hayashi, *J. Appl. Phys.* **102**, 083104 (2007). doi:[10.1063/1.2799049](https://doi.org/10.1063/1.2799049)
12. E. Lioudakis, A. Othonos, I. Alexandrou, Y. Hayashi, *Appl. Phys. Lett.* **91**, 111117 (2007). doi:[10.1063/1.2785120](https://doi.org/10.1063/1.2785120)
13. H. Hoppe, S. Shokhovets, G. Gobsch, *Phys. Status Solidi-Rapid Res. Lett. (RRL)* **1**, R40 (2007)
14. E. Lioudakis, A.G. Nassiopoulou, A. Othonos, *Semicond. Sci. Technol.* **21**, 1041 (2006). doi:[10.1088/0268-1242/21/8/010](https://doi.org/10.1088/0268-1242/21/8/010)
15. E. Lioudakis, A. Othonos, C.B. Lioutas, N. Vouroutzis, *Nanoscale Res. Lett.* **3**, 1 (2008). doi:[10.1007/s11671-007-9105-1](https://doi.org/10.1007/s11671-007-9105-1)
16. E. Lioudakis, K. Adamou, A. Othonos, *Opt. Eng.* **44**, 034203 (2005). doi:[10.1117/1.1873432](https://doi.org/10.1117/1.1873432)
17. E. Lioudakis, A.G. Nassiopoulou, A. Othonos, *Appl. Phys. Lett.* **90**, 171103 (2007). doi:[10.1063/1.2728756](https://doi.org/10.1063/1.2728756)
18. M.J. Biercuk et al., *Appl. Phys. Lett.* **80**, 2767 (2002). doi:[10.1063/1.1469696](https://doi.org/10.1063/1.1469696)
19. F. Wang, M.Y. Sfeir, L. Huang, X.M.H. Huang, Y. Wu, J. Kim et al., *Phys. Rev. Lett.* **96**, 167401 (2006). doi:[10.1103/PhysRevLett.96.167401](https://doi.org/10.1103/PhysRevLett.96.167401)
20. Y.K. Kwon, S. Saito, D. Tomanek, *Phys. Rev. B* **58**, R13314 (1998). doi:[10.1103/PhysRevB.58.R13314](https://doi.org/10.1103/PhysRevB.58.R13314)
21. A.A. Maarouf, C.L. Kane, E.J. Mele, *Phys. Rev. B* **61**, 11 156 (2000)
22. S. Reich, C. Thomsen, P. Ordejon, *Phys. Rev. B* **65**, 155411 (2002). doi:[10.1103/PhysRevB.65.155411](https://doi.org/10.1103/PhysRevB.65.155411)
23. M.J. O'Connell, S. Sivaram, S.K. Doorn, *Phys. Rev. B* **69**, 235415 (2004). doi:[10.1103/PhysRevB.69.235415](https://doi.org/10.1103/PhysRevB.69.235415)
24. R.H. Baughman, A.A. Zakhidov, W.A. de Heer, *Science* **297**, 787 (2002). doi:[10.1126/science.1060928](https://doi.org/10.1126/science.1060928)
25. M.J. O'Connell, S.M. Bachilo, C.B. Huffman, V.C. Moore, M.S. Strano, E.H. Haroz et al., *Science* **297**, 593 (2002). doi:[10.1126/science.1072631](https://doi.org/10.1126/science.1072631)
26. E. Lioudakis, C. Kanari, A. Othonos, I. Alexandrou, *Diamond Relat. Mater.* (2008). doi:[10.1016/j.diamond.2008.01.028](https://doi.org/10.1016/j.diamond.2008.01.028)
27. E. Lioudakis, A. Othonos, *Phys. Status Solidi-Rapid Res. Lett. (RRL)* **2**, 19 (2008). doi:[10.1002/pssr.200701219](https://doi.org/10.1002/pssr.200701219)